

In the format provided by the authors and unedited.

RocS drives chromosome segregation and nucleoid protection in *Streptococcus pneumoniae*

Chryslène Mercy¹, Adrien Ducret^{ID 1}, Jelle Slager², Jean-Pierre Lavergne¹, Céline Freton¹, Sathya Narayanan Nagarajan^{ID 1}, Pierre Simon Garcia¹, Marie-Françoise Noirot-Gros^{3,5}, Nelly Dubarry^{1,6}, Julien Nourikyan^{ID 1}, Jan-Willem Veening^{ID 2,4} and Christophe Grangeasse^{ID 1*}

¹Molecular Microbiology and Structural Biochemistry, UMR 5086, Université Claude Bernard Lyon 1, Centre National de la Recherche Scientifique, Lyon, France. ²Molecular Genetics Group, Groningen Biomolecular Sciences and Biotechnology Institute, Centre for Synthetic Biology, University of Groningen, Groningen, The Netherlands. ³Micalis Institute, UMR1319, INRA, AgroParisTech, Université Paris-Saclay, Jouy-en-Josas, France. ⁴Department of Fundamental Microbiology, Faculty of Biology and Medicine, University of Lausanne, Biophore Building, Lausanne, Switzerland. ⁵Present address: Biosciences Division, Argonne National Laboratory, Lemont, IL, USA. ⁶Present address: Evotec ID, Marcy l'Etoile, France. *e-mail: c.grangeasse@ibcp.fr

Supplementary Information

RocS drives chromosome segregation and nucleoid protection in *Streptococcus*

pneumoniae

Chryslène Mercy¹, Adrien Ducret¹, Jelle Slager², Jean-Pierre Lavergne¹, Céline Freton¹, Sathya Narayanan Nagarajan¹, Pierre Simon Garcia¹, Marie-Francoise Noirot-Gros^{3, #}, Nelly Dubarry^{1, †}, Julien Nourikyan¹, Jan-Willem Veening^{2, 4}, Christophe Grangeasse^{1, *}

This file contains:

- Supplementary Information Guide
- Supplementary Figures with corresponding legends (from S1 to S23)
- Supplementary Video legends (from 1 to 4)
- Supplementary Tables (S1 and S2) with corresponding legends

SUPPLEMENTARY INFORMATION GUIDE

Supplementary Figure 1: Analysis of the interaction between CpsD and Spr0895 (RocS)

Supplementary Figure 2: Taxonomic distribution of RocS in Lactobacillales

Supplementary Figure 3: Production of capsular polysaccharides (CPS)

Supplementary Figure 4: Growth and cell shape analysis of D39 and $\Delta rocS$ strains

Supplementary Figure 5: Impact of *rocS* deletion on nucleoid distribution and cell-shape of D39 Δcps cells

Supplementary Figure 6: Impact of *rocS* deletion on nucleoid distribution, cell-growth and cell-shape of R800 cells

Supplementary Figure 7: Deletion of *rocS* and *parB* or *rocS* and *smc* have a cumulative detrimental effect on the viability of the pneumococcus

Supplementary Figure 8: Localization of GFP-FtsA in WT and $\Delta rocS$ R800 strains

Supplementary Figure 9: Marker frequency analysis of the *oriC* and *ter* regions

Supplementary Figure 10: Validation of strains expressing the *oriC* localization system

Supplementary Figure 11: Growth curves and nucleoid distribution of cells producing GFP and FLAG fusions

Supplementary Figure 12: Expression of *rocS* fusions

Supplementary Figure 13: GFP-RocS forms both bright foci and highly dynamic faint foci

Supplementary Figure 14: Co-localization of RepC-mKate2 and GFP-RocS in R800 cells

Supplementary Figure 15: Interaction between RocS and ParB

Supplementary Figure 16: Bioinformatic analysis of the amino acid sequence of RocS

Supplementary Figure 17: Growth curves and cell viability of *rocS-ΔAH* and *ΔHTH-rocS* mutants

Supplementary Figure 18: ChIP-seq analysis of GFP-RocS binding on the *Streptococcus pneumoniae* genome

Supplementary Figure 19: RocS directly interacts with the DNA *in vitro*

Supplementary Figure 20: Impact of RocS overproduction on pneumococcal cell shape and nucleoid distribution

Supplementary Figure 21: Co-localization of CpsD-mKate2 and GFP-RocS in D39 cells

Supplementary Figure 22: Interaction between RocS and FtsZ

Supplementary Figure 23: Full images of immunoblots and SDS-PAGE used in this study

Supplementary Video 1: Nucleoid segregation in wild-type R800 cells

Supplementary Video 2: Absence of chromosome segregation in $\Delta rocS$ cells

Supplementary Video 3: Chromosome pinching in $\Delta rocS$ cells

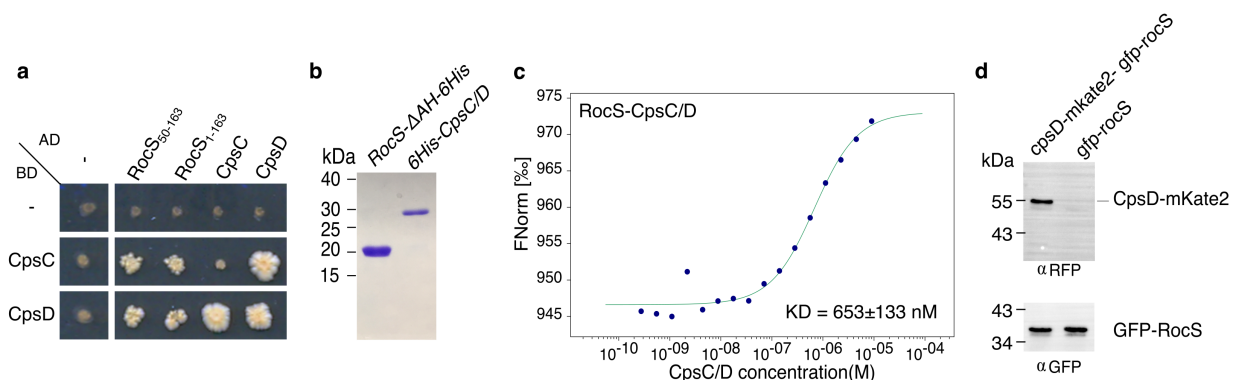
Supplementary Video 4: Localization of GFP-RocS

Supplementary Table 1: Strains and plasmids

Supplementary Table 2: List of Primers

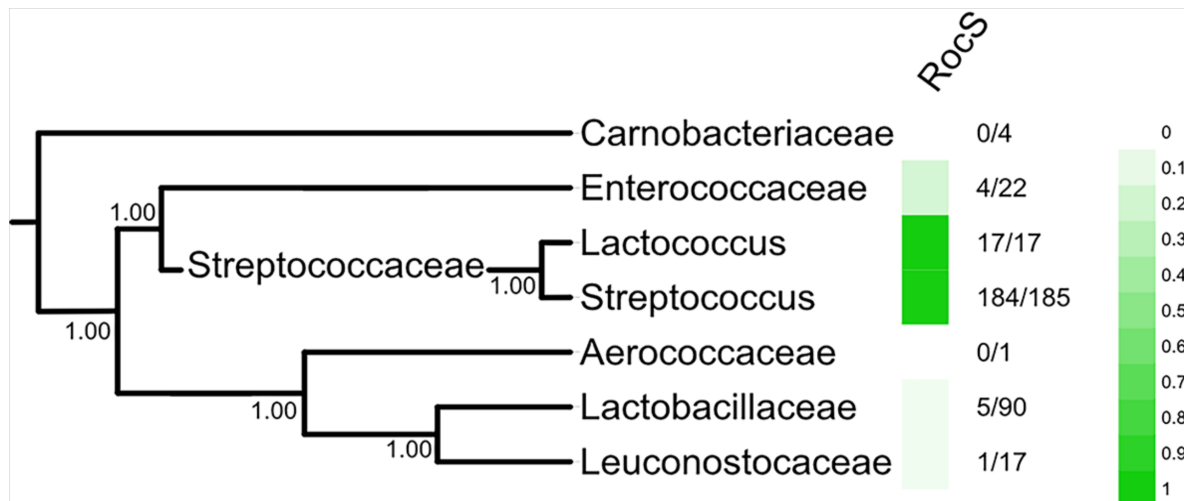
Supplementary Figure 1: Analysis of the interaction between CpsD and Spr0895 (RocS)

a. Protein-protein interaction between RocS (Spr0895) CpsD or CpsC assayed by yeast two-hybrid. AD and BD refer to activating and DNA-binding domain of Gal4 fused to either CpsD, RocS(50-163), RocS(1-163), or CpsC, and CpsD or CpsC, respectively. The minimal interacting domain necessary for RocS interaction with CpsD or CpsC was delineated from residue 50 to 163. Protein-protein interactions were assayed by the ability of the diploids to grow on SC-LUH selective media (without histidine). (-) indicates empty vectors, used as negative controls. Interaction between BD-CpsD and AD-CpsC or AD-CpsD were used as positive controls as previously reported. **b.** Protein purification. The chimera CpsC/D and RocS- Δ AH (RocS devoid of the C-terminal amphipatic helix, see Supplementary Fig. 15) were overproduced in *E. coli* as 6His-tagged fusion proteins. After purification using a Ni-NTA resin, 6His-CpsC/D and RocS- Δ AH-6His were analyzed by SDS-PAGE. **c.** Affinity measurements by Microscale Thermophoresis of labeled RocS- Δ AH-6H binding to increasing concentrations of 6His-CpsC/D chimera. FNorm (normalized fluorescence) is plotted as a function of ligand concentration. Measurements are represented by blue dots and the fitted curve by a green line. KD is expressed at the mean \pm SD **d.** Immunoprecipitation of CpsD-mKate2 with GFP-RocS in *gfp-rocs-CpsD-mkate2* and *gfp-rocs* strains using anti-GFP antibodies. Samples were analyzed by immunoblotting using either anti-GFP antibodies (lower panel) to check that the same amount of RocS was loaded, or anti-mKate2 antibodies (upper panel) to determine the presence of co-immunoprecipitated CpsD-mKate2. The data shown are representatives of experiments made independently in triplicate.



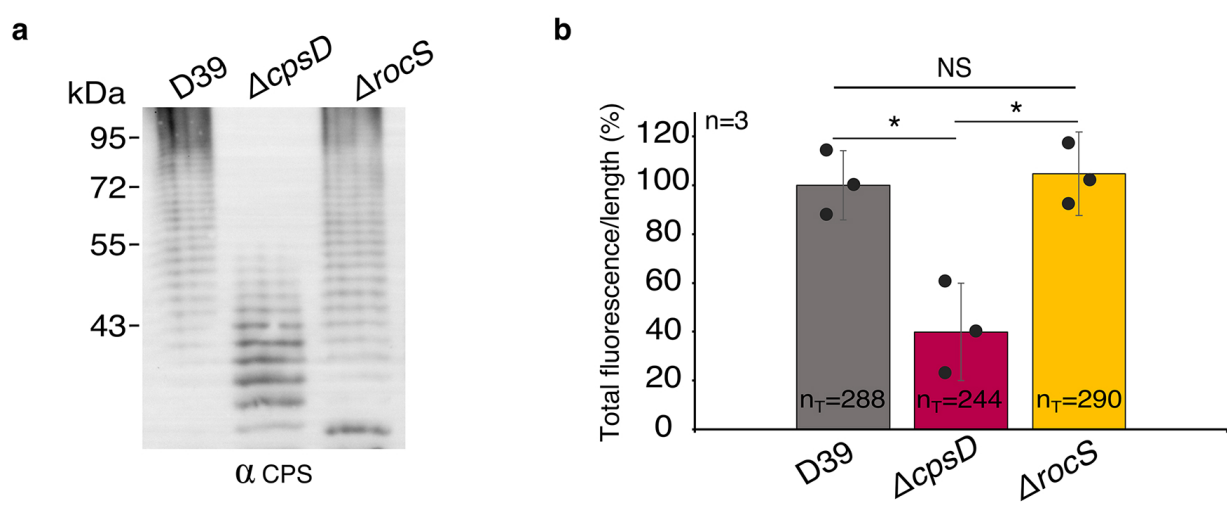
Supplementary Figure 2: Taxonomic distribution of RocS in Lactobacillales

The number of species containing a RocS homolog compared with the total number of sequenced species in the genera are indicated. The relative proportion of genomes containing at least one copy of *rocS* is color-coded using a green scale.



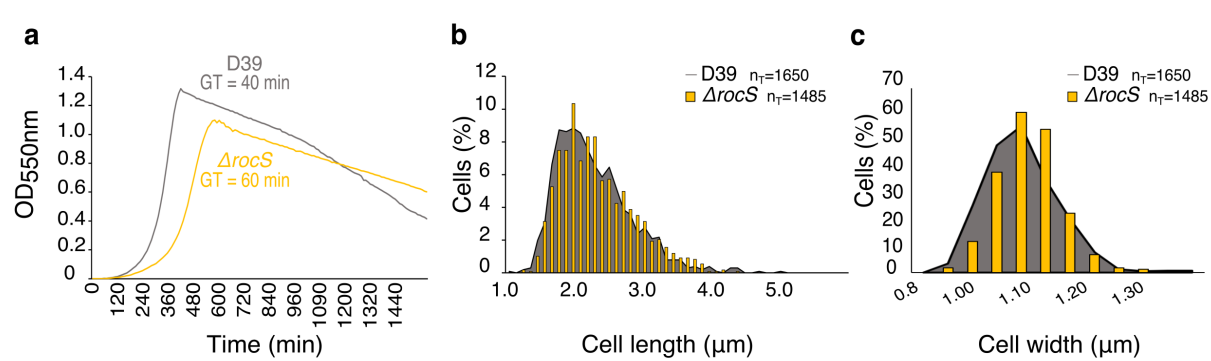
Supplementary Figure 3: Production of capsular polysaccharides (CPS)

a. Detection of cell-associated CPS in the D39 strain and the $\Delta cpsD$ and $\Delta rocS$ derivatives. The same volume of CPS prepared from culture grown until $OD_{550} = 0.3$ was loaded in each lane. The immunoblot was probed with a rabbit anti-serotype 2 CPS polyclonal antibody. **b.** Quantification of the CPS fluorescent signal in living D39, $\Delta cpsD$ and $\Delta rocS$ strains, normalized by the average amount of fluorescent signal detected for D39. Bar chart, with data points overlap, represents the mean \pm SEM. P -values derived from a two-sided Mann-Whitney rank sum test performed between the following pairs: ‘D39’ vs ‘ $\Delta cpsD$ ’ ($P=3.68 \cdot 10^{-2}$), ‘D39’ vs ‘ $\Delta rocS$ ’ ($P=1.3$) and ‘ $\Delta cpsD$ ’ vs ‘ $\Delta rocS$ ’ ($P=1.5 \cdot 10^{-2}$). * $P < 0.001$. ns $P > 0.05$. n_T indicates the number of cells analyzed. **a-b.** The data shown are representatives of experiments made independently in triplicate ($n=3$).



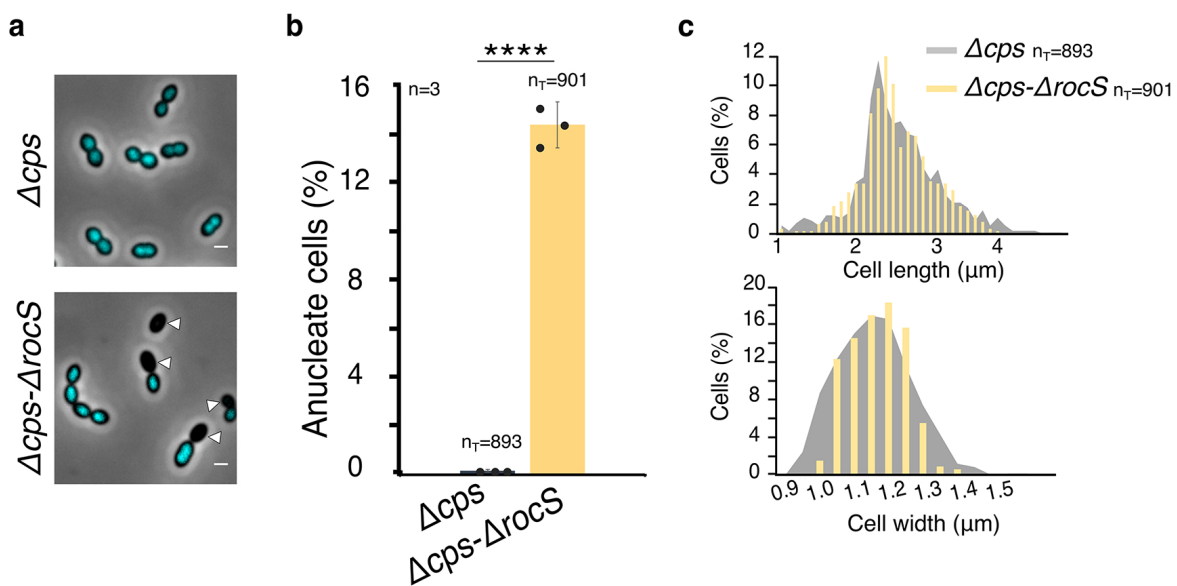
Supplementary Figure 4: Growth and cell shape analysis of D39 and $\Delta rocS$ strains

a. Representative growth curves for the D39 strain and the $\Delta rocS$ derivative. Strains were grown in CH+Y medium at 37 °C in a JASCO V-630 Biospectrophotometer. The OD₅₅₀ was read automatically every 10 min. The curves shown in (a) are representative of three replicates. GT stands for generation time. **b-c.** Cell length (b) and width (c) distribution of D39 and $\Delta rocS$ cells. n_T indicates the total number of cells analyzed. Experiments were independently performed in triplicate.



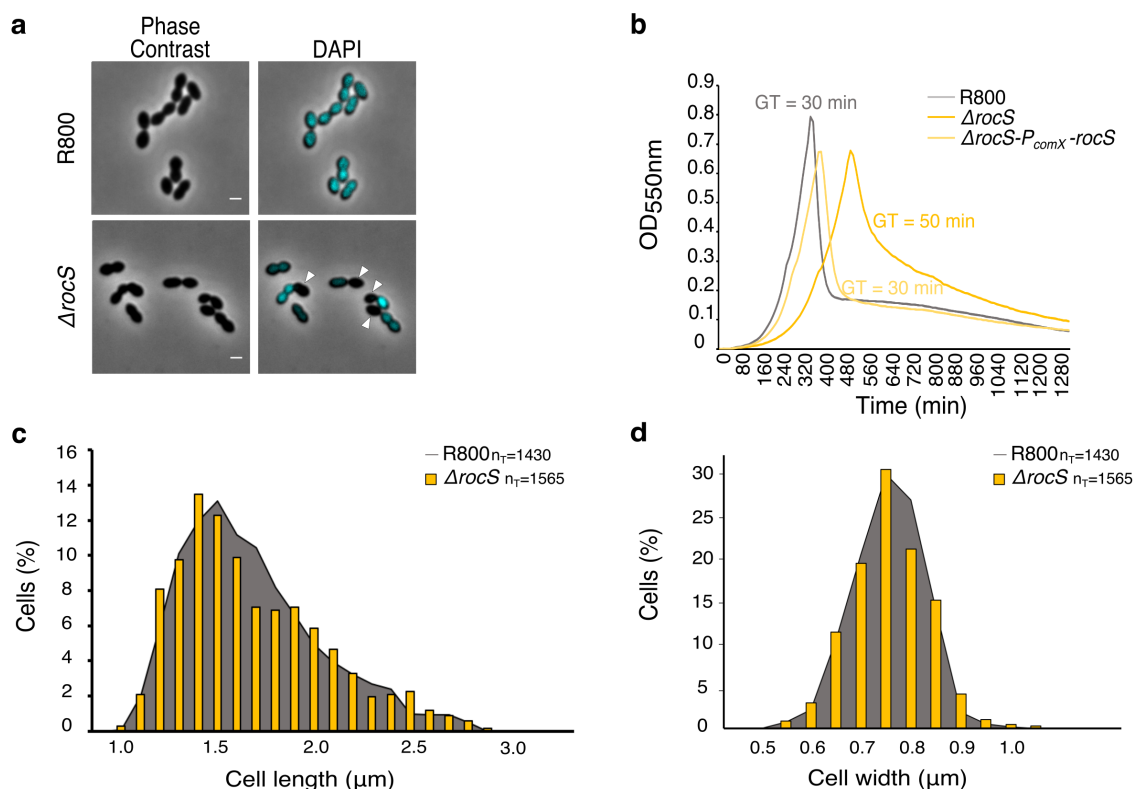
Supplementary Figure 5: Impact of *rocS* deletion on nucleoid distribution and cell-shape of D39 Δ *cps* cells

a. Visualization of nucleoids in the D39 Δ *cps* strain and the Δ *rocS* derivative. Localization of nucleoids was analyzed using DAPI staining. Merged images between phase contrast and DAPI fluorescent signal are shown. Arrowheads indicate anucleate cells. Scale bar, 1 μ m. **b.** The percentage of anucleate cells in the D39 Δ *cps* strain and the Δ *rocS* derivative. Bar chart, with data points overlap, represents the mean \pm SD. Two-tailed *P*-values derived from a two-population proportion test for the following pair: ‘D39- Δ *cps*’ vs ‘D39- Δ *rocS*’ ($P<0.0001$). **** $P < 0.0001$. **c.** Distribution of the cell length and cell width from D39 Δ *cps* and D39 Δ *cps* Δ *rocS* cells. n_T indicates the total number of cells analyzed. Experiments were independently performed in triplicate.



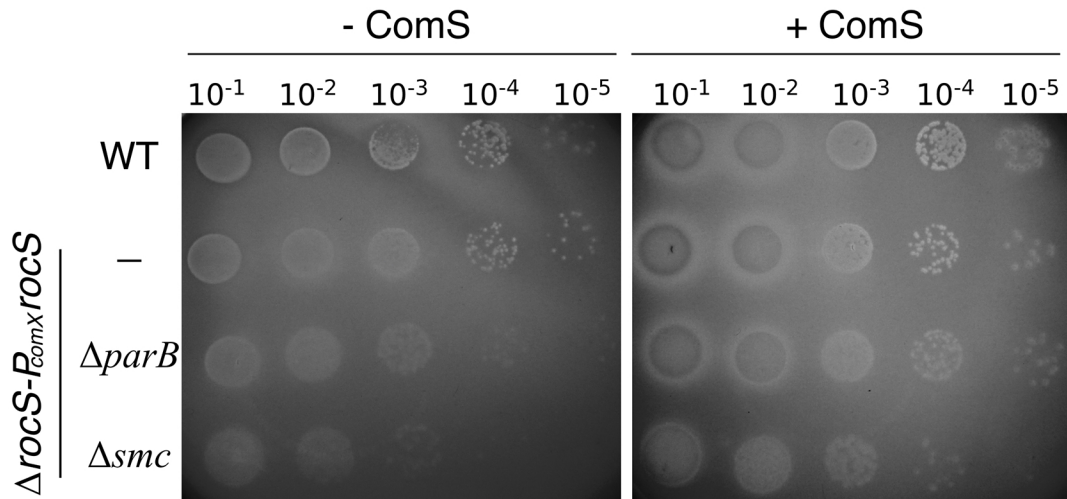
Supplementary Figure 6: Impact of *rocS* deletion on nucleoid distribution, cell-growth and cell-shape of R800 cells

a. Visualization of nucleoids in the R800 strain and the $\Delta rocS$ derivative. Localization of nucleoids was analyzed using DAPI staining. Phase contrast (left column) and merged images between phase contrast and DAPI fluorescent signal (right column) are shown. Arrowheads indicate anucleate cells. Scale bar, 1 μm . **b.** Representative growth curves for the R800 strain, the $\Delta rocS$ derivative and the complementation strain. Strains were grown in CH+Y medium at 37 °C in a JASCO V-630 Biospectrophotometer. The OD₅₅₀ was measured automatically every 10 min. GT stands for generation time. **c-d.** Cell length (c) and width (d) distribution of R800 and $\Delta rocS$ cells. n_T indicates the total number of cells analyzed. **a-d.** Experiments were performed in triplicate.



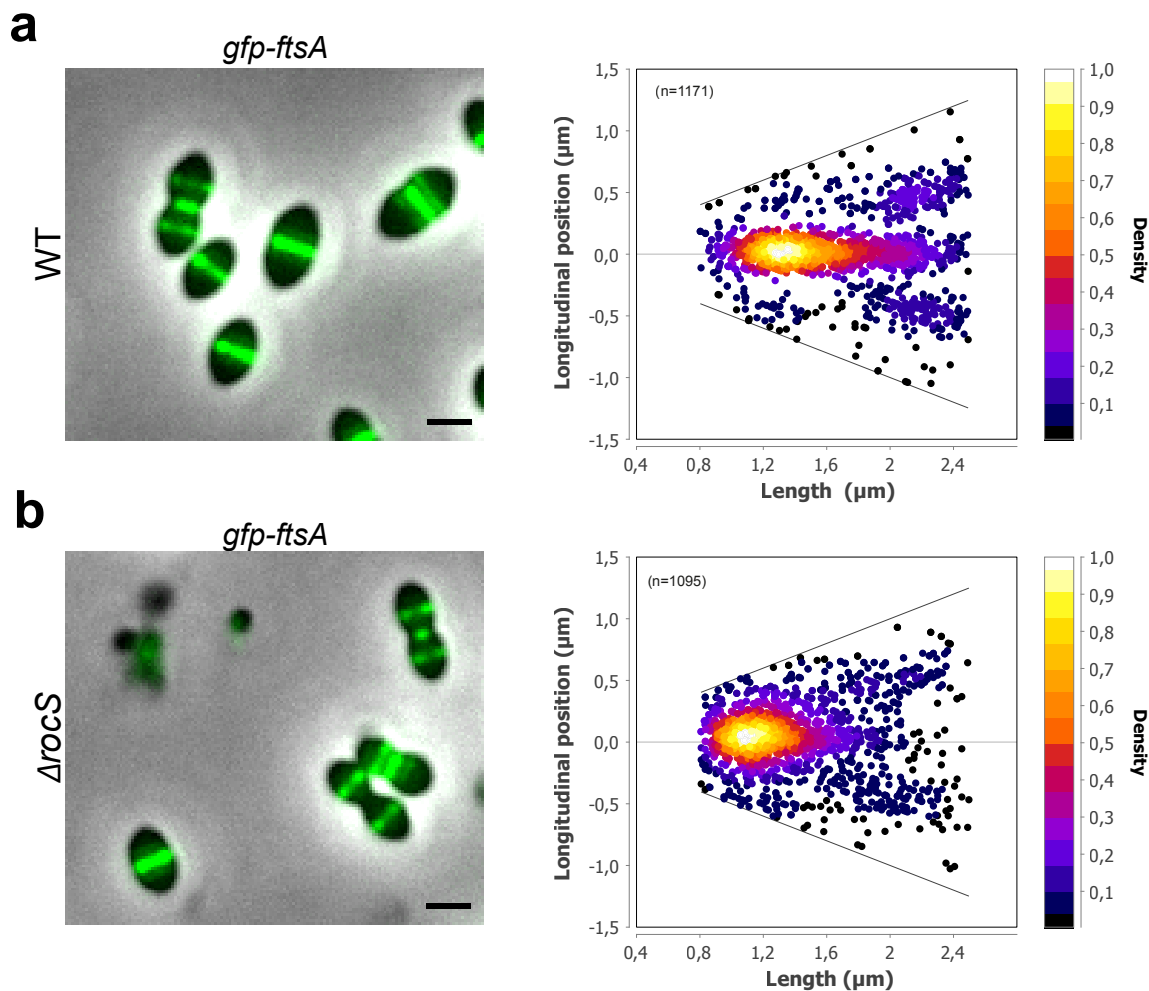
Supplementary Figure 7: Deletion of *rocS* and *parB* or *rocS* and *smc* have a cumulative detrimental effect on the viability of the pneumococcus

S. pneumoniae D39 strains were grown to exponential phase and normalized to an OD₆₀₀ of 0.2. Resulting cultures were serially diluted and 10 µl of each dilution spotted onto THY horse blood plates in the presence or absence of 0.1 µM ComS. Plates were then incubated at 37°C. The absence of *rocS* decreases the viability of *smc* and *parB* mutant by > 1 log₁₀ levels. Images are representative of 3 experiments repeated independently.



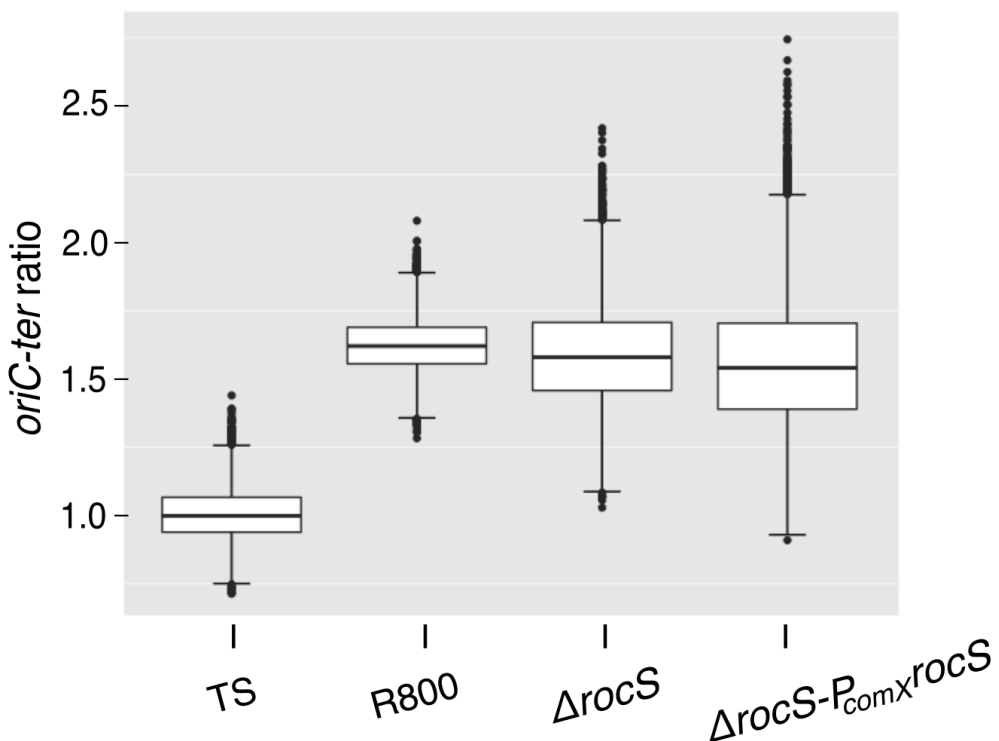
Supplementary Figure 8: Localization of GFP-FtsA in WT and $\Delta rocS$ R800 strains.

a-b. Representative merged images between phase contrast and GFP fluorescence signal of (a) R800 or (b) $\Delta rocS$ R800 cells expressing the *gfp-ftsA* fusion. Scale bar, 1 μm . The corresponding heat maps representing the longitudinal localization of GFP-FtsA as a function of the cell length in WT or $\Delta rocS$ R800 cells are shown on the right. GFP-FtsA localized at mid-cell and at the future sites of division in WT and in $\Delta rocS$ cells. Due to an over-representation of small cells in the $\Delta rocS$ strain, GFP-FtsA was observed more frequently at mid-cell in $\Delta rocS$ cells. n indicates the total number of cells analyzed from one experiment. Images and Heatmaps are representative of 3 experiments repeated independently.



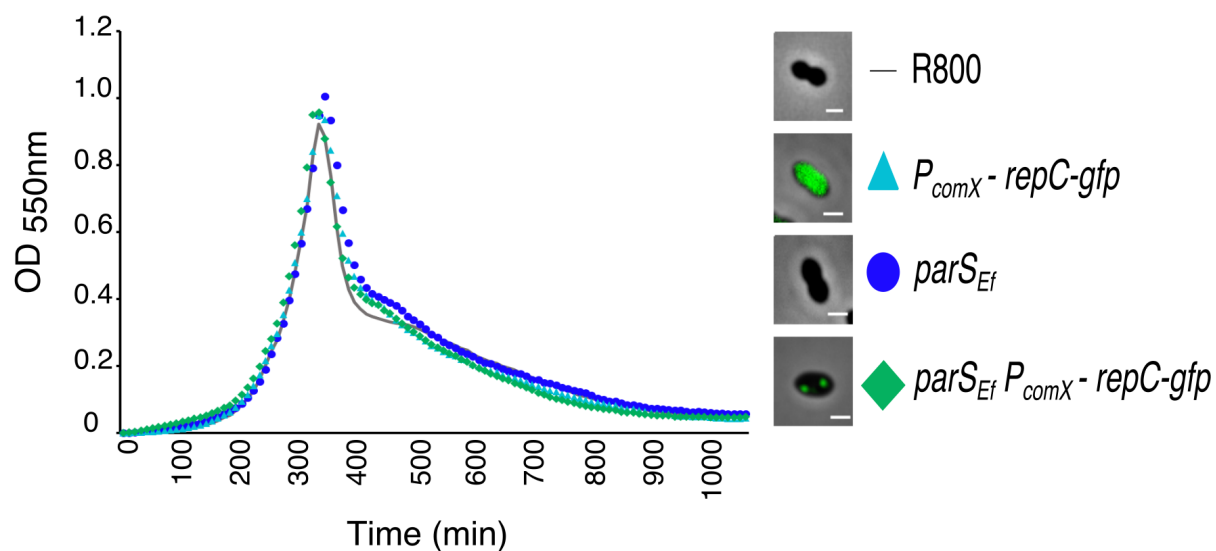
Supplementary Figure 9: Marker frequency analysis of the *oriC* and *ter* regions

Boxplot representing the ratio between the origin of replication (*oriC*) and the terminus region (*ter*) of the chromosome determined by real-time qPCR of chromosomal DNA isolated from exponentially growing ΔrocS and $\Delta\text{rocS-P}_{\text{comX}}\text{-rocS}$ cells. Results are from 10,000 Monte Carlo simulations based on n=7 replicate measurements. As controls, the *oriC/ter* ratio was determined for R800 cells and for a thermo-sensitive *dnaA-T1193C* (DnaA-M398T) mutant (TS). Box indicates the 25th to 75th percentile and whiskers are at 1.5 x IQR (interquartile range) of data from Monte Carlo simulations. Dots are all outliers.



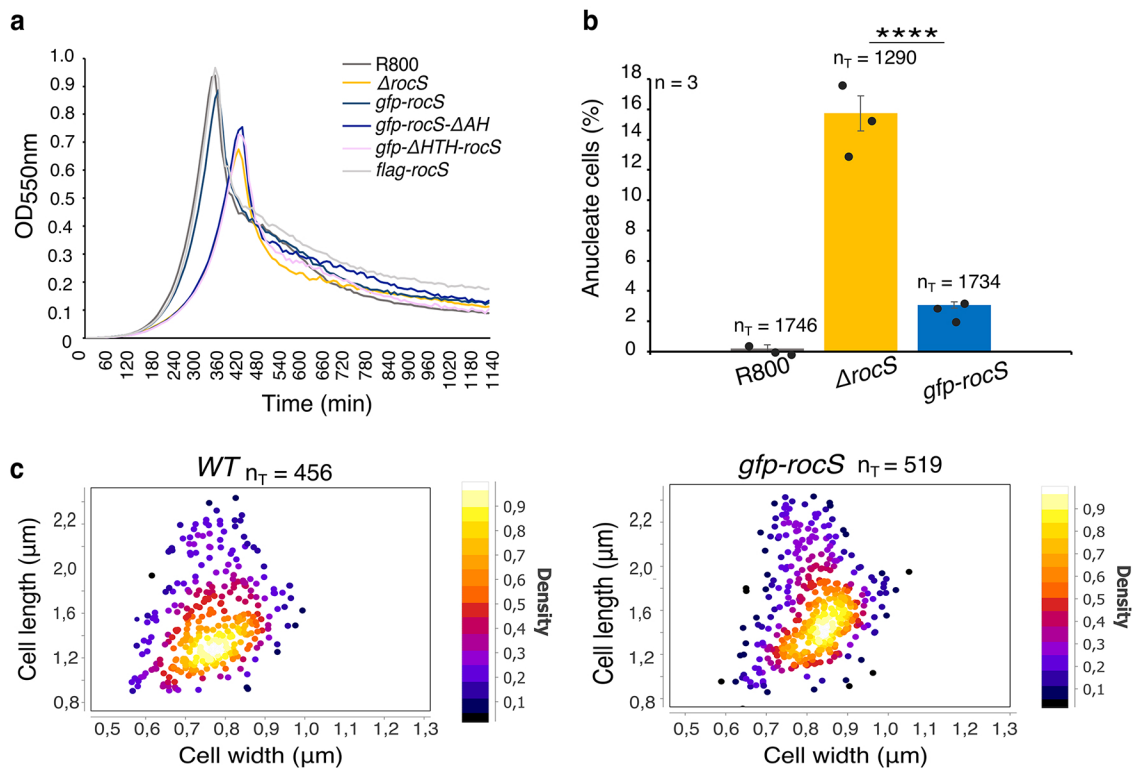
Supplementary Figure 10: Validation of strains expressing the *oriC* localization system

Representative growth curves for the R800 strain and P_{comX} -*repC-gfp*, $parS_{Ef}$ and $parS_{Ef} P_{comX}$ -*repC-gfp* derivatives. Strains were grown in CH+Y medium at 37 °C in a JASCO V-630 Biospectrophotometer. The OD₅₅₀ was measured automatically every 10 min. Curves are representative of three replicates. Overlays between phase contrast and GFP fluorescence signal are shown on the right to illustrate that the cell shape is not affected and that RepC-GFP localized either in the cytoplasm or as 2 bright foci in the absence or presence of $parS_{Ef}$ sites, respectively. Scale bar: 1 μm.



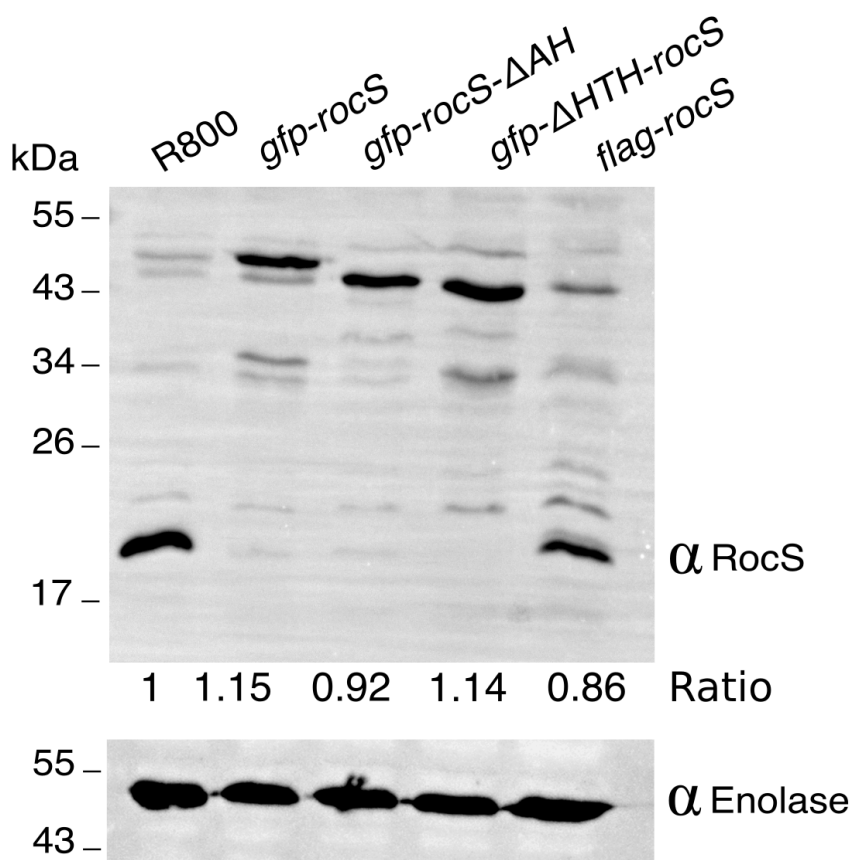
Supplementary Figure 11: Growth curves and nucleoid distribution of cells producing GFP and FLAG fusions

a. Growth curves of R800 (grey) and $\Delta rocS$ cells (orange) and cells expressing either *gfp-rocS* (dark blue), *gfp-rocS-ΔAH* (light blue), *gfp-ΔHTH-rocS* (light orange) or *flag-rocS* (light grey) in CH+Y medium at 37 °C. The OD₅₅₀ was measured automatically every 10 min. All fusion proteins are the only source of RocS, RocS-ΔAH and ΔHTH-RocS in cells. The fusion genes encoding these proteins substitute the corresponding native genes at their chromosomal locus. **b.** Percentage of anucleate cells in R800, $\Delta rocS$ and *gfp-rocS* strains. n_T indicates the number of cells analyzed from n=3 independent experiments. Bar chart, with data points overlap, represents the mean ± SEM. Two-tailed P-values derived from a two-population proportion test for the following pair: ‘ $\Delta rocS$ ’ vs ‘*gfp-rocS*’ ($P<0.0001$). **** $P<0.0001$. **c.** Cell size parameters presented as heat maps in which cell width distribution is shown as a function of the cell length of R800 and *gfp-rocS* cells. n_T indicates the total number of cells analyzed. Experiments were independently performed in triplicate.



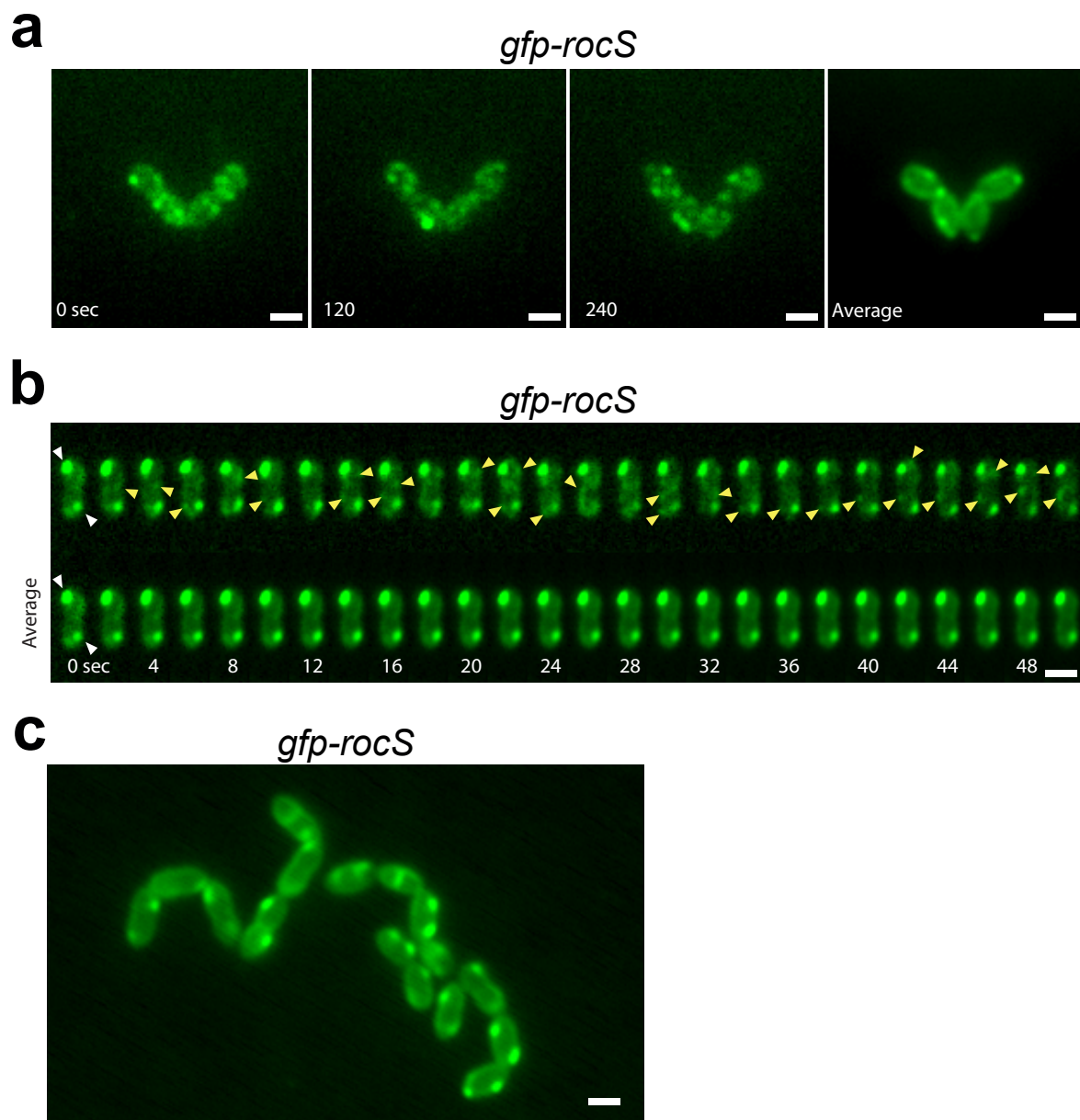
Supplementary Figure 12: Expression of *rocS* fusions

The Western immunoblot was probed with specific anti-RocS antibodies (α RocS) to determine *rocS* expression in R800, *gfp-rocS*, *gfp-rocS-ΔAH*, *gfp-ΔHTH-rocS* and *flag-rocS* cells. To estimate the relative quantity of proteins in crude extract and to compare the different lanes, we used enolase (Spr1036) as an internal standard. The enolase was detected using specific antibodies (α Enolase) and is presented in the lower part of the figure. The numbers under each lane indicate the ratio between the signal of the band corresponding to RocS in the mutant strain and the WT R800 (α RocS/ α RocS-R800) corrected by the signal of the band corresponding to the enolase. RocS is produced at similar levels in the different strains analyzed. Images are representative of 3 experiments repeated independently.



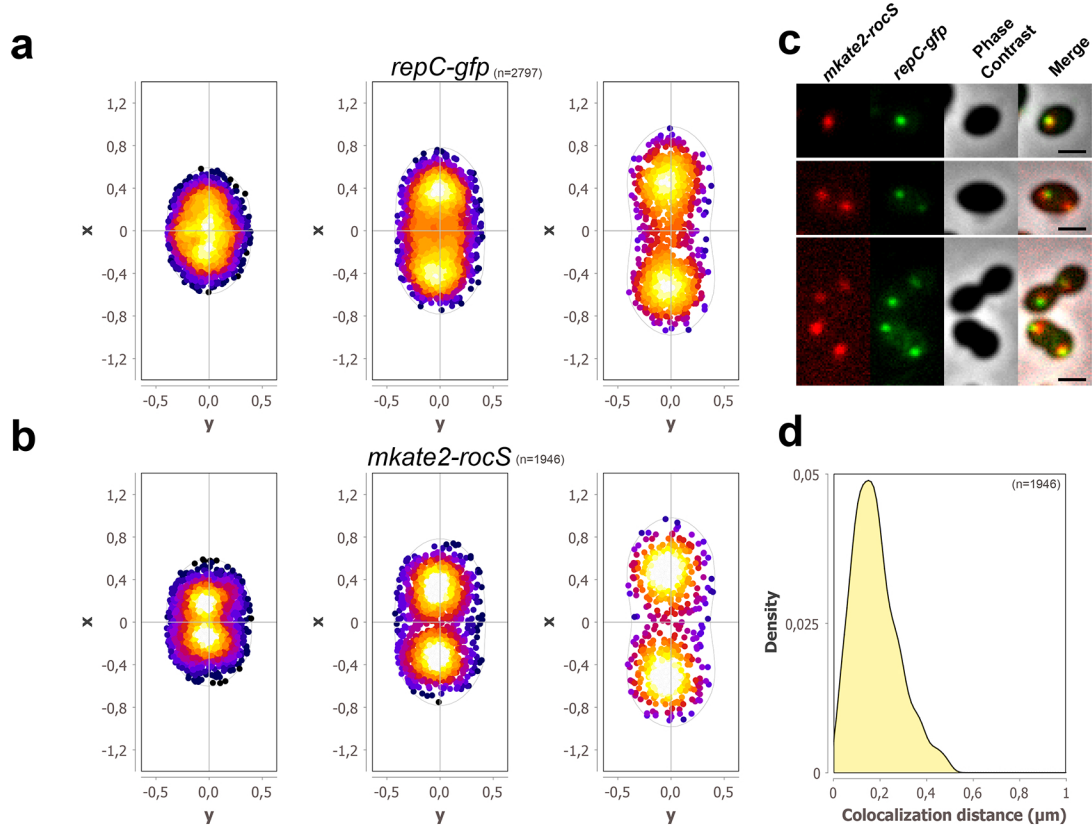
Supplementary Figure 13: GFP-RocS forms both bright foci and highly dynamic faint foci.

a-b. Dynamic localization of the GFP-RocS fusion protein in R800 cells, observed by total internal reflection fluorescence microscopy. **a.** Selected fields of the GFP fluorescence signal and the averaged GFP fluorescence from Movie S4. Image averaging was performed over 20 frames captured every 100 ms. Scale bar, 1 μ m. **b.** Time-lapse montage showing the dynamic of the GFP-RocS fusion protein in a single cell. The GFP-RocS fusion protein forms both bright foci (white triangle) and highly dynamic foci (yellow triangle). The GFP fluorescence signal and the averaged GFP fluorescence signal are shown in the upper and the lower panel, respectively. Scale bar, 1 μ m. **c.** Representative averaged GFP fluorescence signal of R800 cells expressing the GFP-RocS fusion. Image averaging was performed over 50 frames captured every 2 sec. Scale bar, 1 μ m. **a-c.** Images are representative of 3 experiments repeated independently.



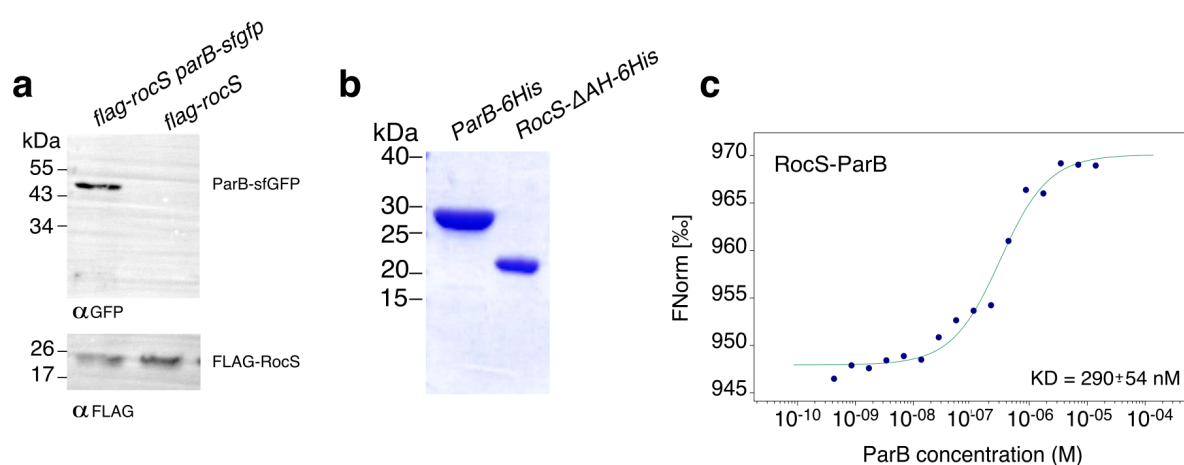
Supplementary Figure 14: Co-localization of RepC-mKate2 and GFP-RocS in R800 cells

a-b. Heat map representing the 2-dimensional localization patterns of (a) RepC-GFP, as a proxy for *OriC*, and (b) mKate2-RocS in R800 cells expressing both fusions. n indicates the number of foci analyzed. **c.** Representative images of phase contrasts, GFP and mKate2 fluorescence signals. The merged image is also shown. Scale bar, 1 μm . **d.** Density plot of the distance measured between RepC foci and the closest RocS foci. n indicates the number of pairs analyzed. Experiments were repeated independently three times with similar results.



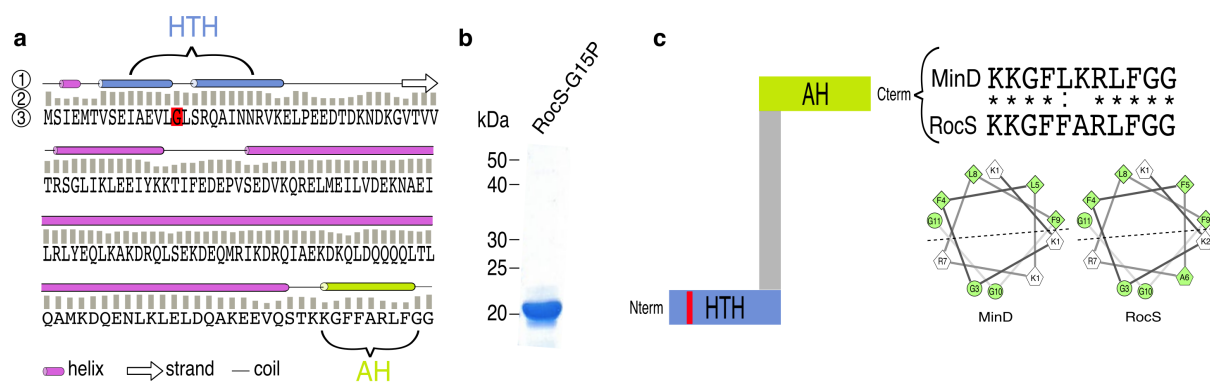
Supplementary Figure 15: Interaction between RocS and ParB

a. Immunoprecipitation of ParB-sfGFP (10) with FLAG-RocS in *flag-rocS-parB-sfgfp* and *flag-rocS* strains using anti-FLAG antibodies (α FLAG). Samples were analyzed by immunoblotting using either anti-FLAG antibodies (lower panel) to check that the same amount of RocS was loaded, or anti-GFP antibodies (upper panel) to determine the presence of co-immunoprecipitated ParB-sfGFP. **b.** Protein purification. ParB and RocS- Δ AH were overproduced in *E. coli* as 6His-tagged fusion proteins. After purification using a Ni-NTA resin, ParB-6His and RocS- Δ AH-6His were analyzed by SDS-PAGE. **c.** Affinity measurements by Microscale Thermophoresis of labeled RocS- Δ AH-6His binding to increasing concentrations of ParB-6His. FNorm (normalized fluorescence = fluorescence after thermophoresis / initial fluorescence) is reported on the y-axis and ligand concentrations on the x-axis are plotted in Molar. Measures are represented by blue dots and fitted curves by green lines. KD is expressed at the mean \pm SD. The data shown are representative of experiments made independently in triplicate.



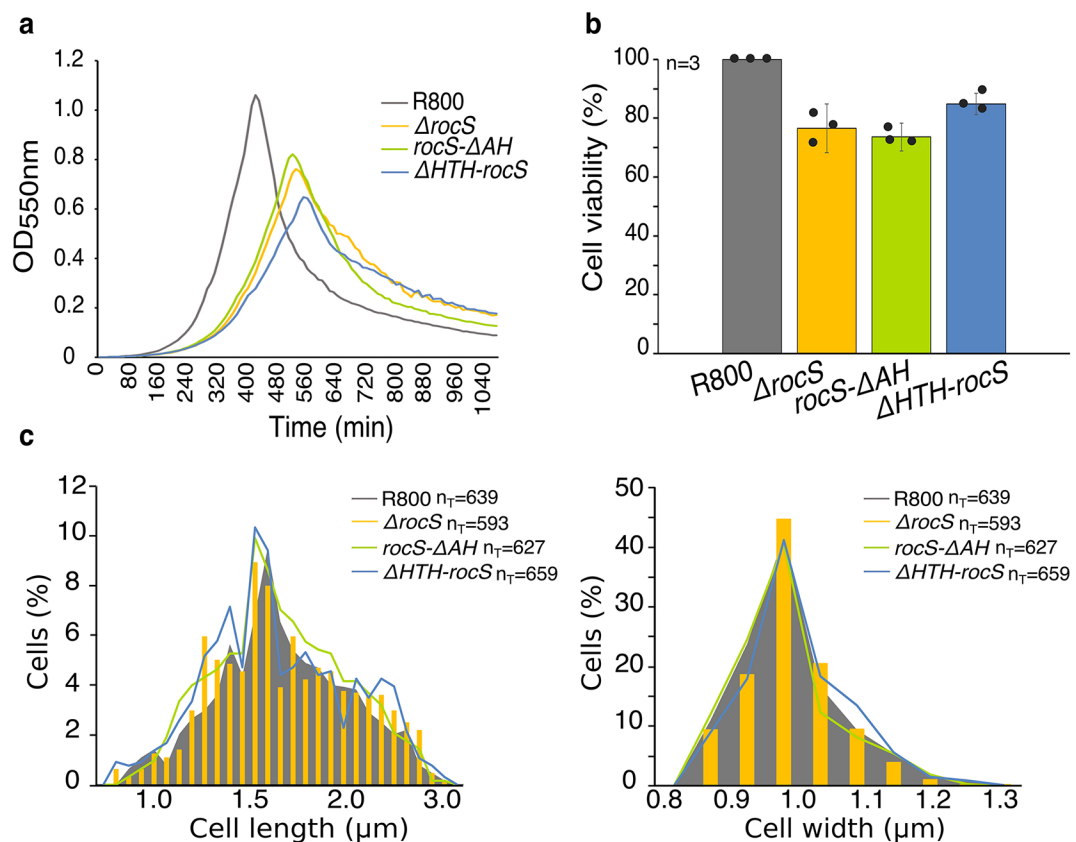
Supplementary 16: Bioinformatic analysis of the amino acid sequence of RocS

a. Secondary structure prediction of RocS using PSIPRED⁴⁶. The prediction of an N-terminal Helix-Turn-Helix domain (HTH) and a C-terminal amphipathic helix (AH) is shown in blue and green, respectively. Digits 1, 2 and 3 in circles show the predicted secondary structure, the confidence of prediction and the RocS sequence, respectively. The conserved glycine 15 of the HTH is indicated by the red box. **b.** Purification of RocS-ΔAH (RocS devoid of the C-terminal amphipathic helix) carrying the glycine 15 to proline mutation. After overproduction in *E. coli* cells as an 6His-tagged fusion, RocS-G15P-ΔAH-6His was purified using a Ni-NTA resin and analyzed by SDS-PAGE. **c.** Schematic representation of RocS with the N-terminal Helix-Turn-Helix in blue and the C-terminal amphipathic helix in green. The conserved glycine in the HTH domain is marked in red. The central predicted α -helix is shown in grey. Sequence alignment and helical representation of the amphipathic helices of RocS and MinD of *E. coli*²¹ are shown on the right. Non-polar residues are shown in green. The strong conservation of the amino acids in the upper-side of each helix indicate that the C-terminal amphipathic helix of RocS interacts with the membrane.



Supplementary Figure 17: Growth curves and cell viability of *rocS*-*ΔAH* and *ΔHTH-rocS* mutants

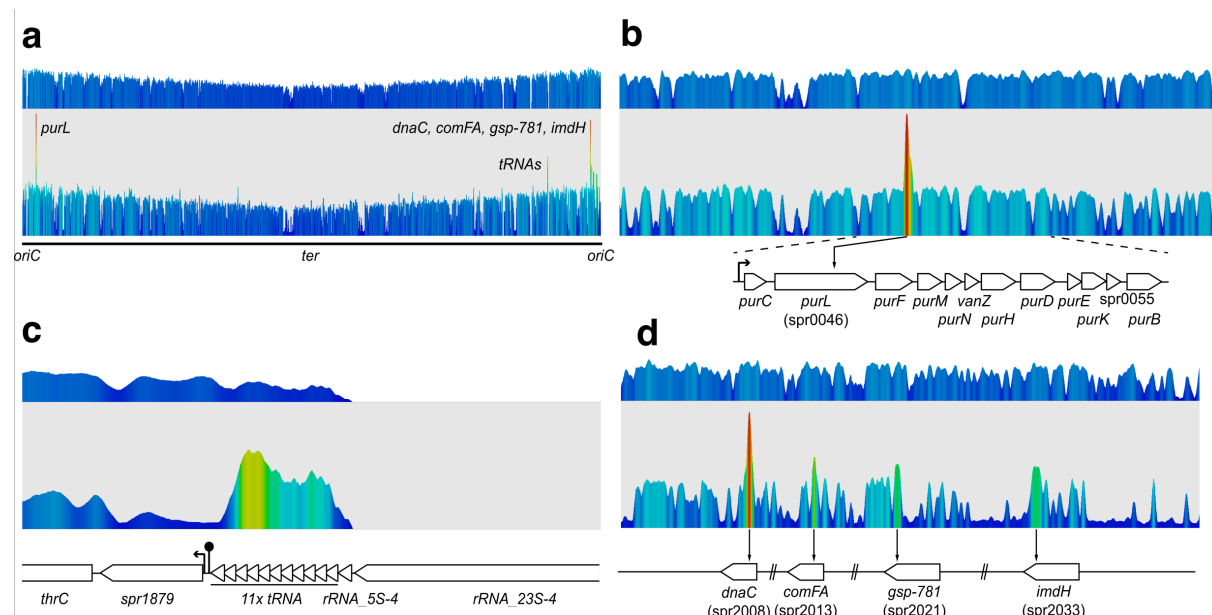
a. Growth curves of R800 (grey), $\Delta rocS$ (orange), *rocS*-*ΔAH* (green), or *ΔHTH-rocS* (dark blue) strains in CH+Y medium at 37 °C. The OD_{550nm} was measured automatically every 10min. **b.** Relative cell viability of $\Delta rocS$ (orange), *rocS*-*ΔAH* (green), or *ΔHTH-rocS* (dark blue) strains compare to WT (R800 grey). Bar chart, with data points overlap, represents the mean ± SEM. **c-d.** Cell length (c) and width (d) distribution of R800 and *rocS* mutant strains. n_T indicates the total number of cells analyzed. Each experiment was performed independently in triplicate (n=3).



Supplementary Figure 18: ChIP-seq analysis of GFP-RocS binding on the *Streptococcus pneumoniae* genome.

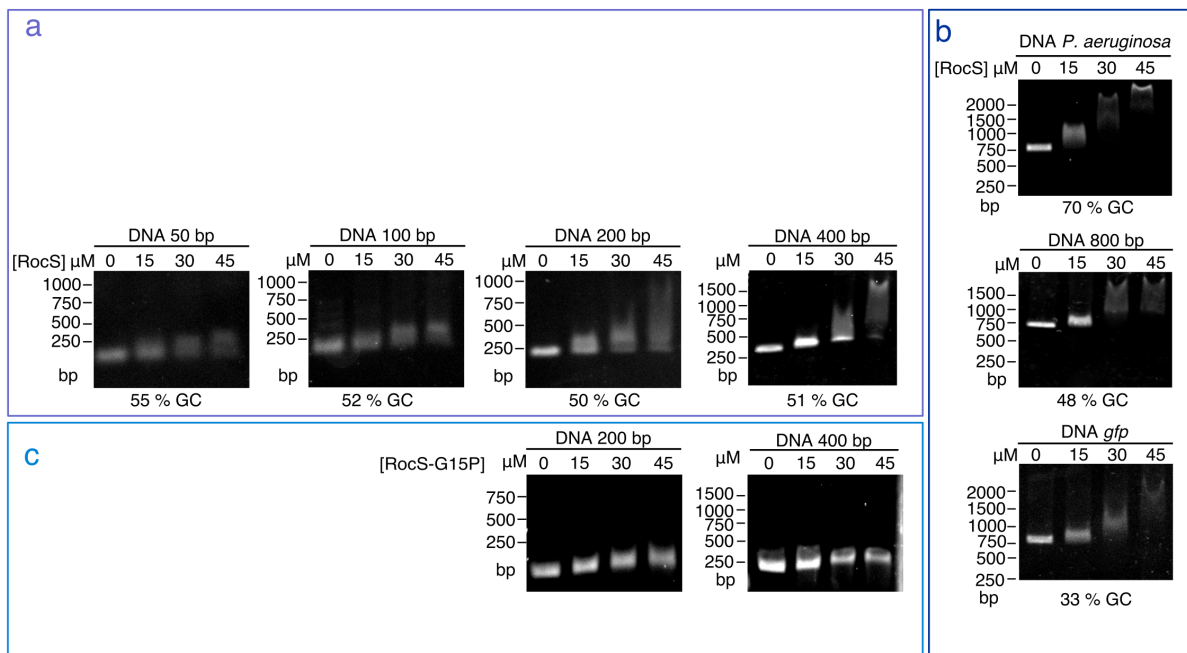
The protocol for immunoprecipitation of FLAG-tagged RocS was performed in duplicate. ChIP-seq coverage after immunoprecipitation of FLAG-tagged RocS, visualized by SeqMonk (<https://www.bioinformatics.babraham.ac.uk/projects/seqmonk>). Relevant transcription start sites and terminators were predicted based on sequence identity with *S. pneumoniae* D39V⁴⁸.

a. Genome-wide coverage of the *S. pneumoniae* R6 genome. **b.** Coverage of *purL* locus (spr0045-spr0056 are drawn). **c.** Coverage of a tRNA cluster (sprt43-sprt53). Note that reads mapping to rRNA (sprr11) are ignored due to multiple mapping sites. **d.** Coverage of genomic region containing *dnaC*, *comFA*, *gsp-781* and *imdH*. For each of the regions mentioned above, 500 nucleotides around the center of the peak were extracted and used to look for possibly enriched motifs using the Meme-chip tool (<http://meme-suite.org/tools/meme-chip>). No significantly enriched motifs were found.



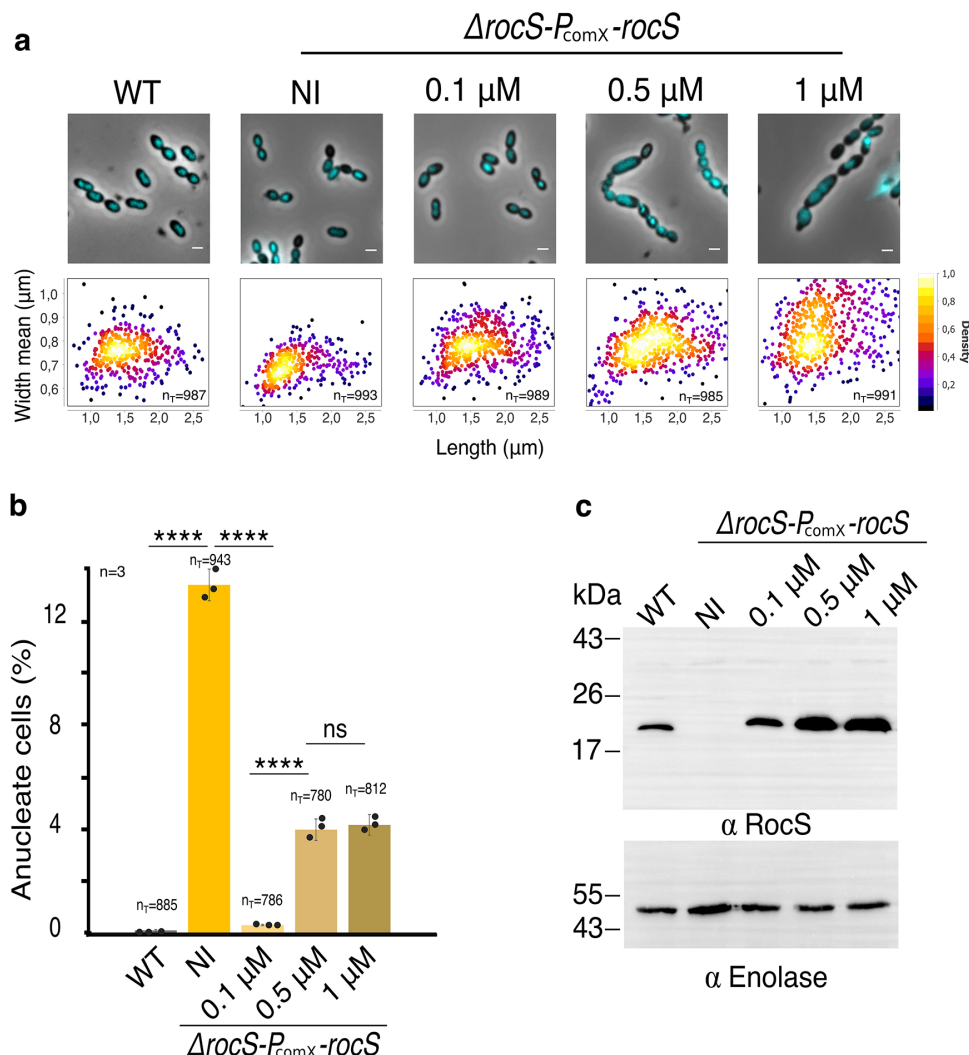
Supplementary Figure 19: RocS directly interacts with the DNA *in vitro*

Electrophoretic mobility shift assays (EMSA) on agarose gels stained with ethidium bromide and developed under UV light. The indicated concentrations of purified RocS-ΔAH-6His were incubated with DNA fragments (50 ng) (a) of different lengths (50, 100, 200, 400 or 800 bp) and (b) GC contents (all fragments are 800 bp in length). c. same as in (a) but EMSA were performed with RocS-G15P-ΔAH-6His. The data shown are representative of experiments made independently in triplicate.



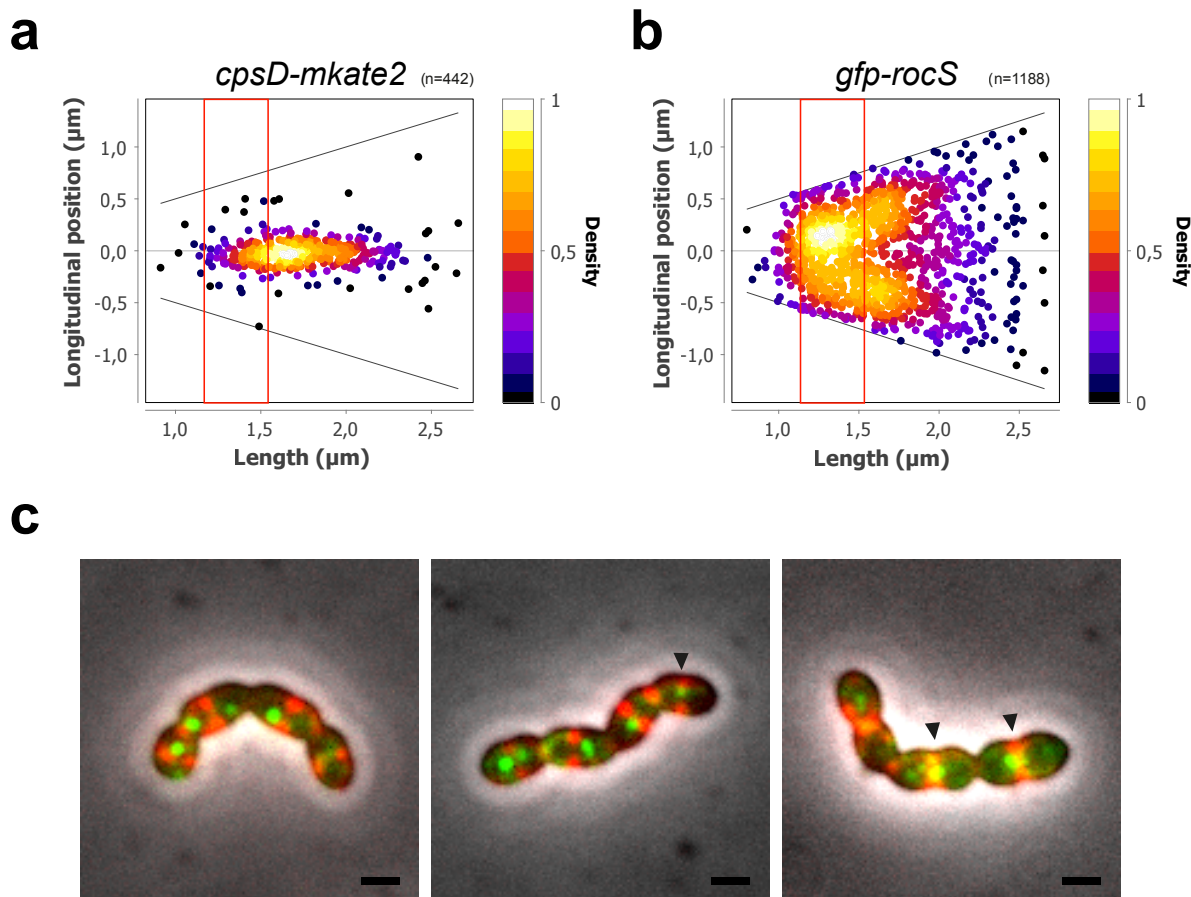
Supplementary Figure 20: Impact of RocS overproduction on pneumococcal cell shape and nucleoid distribution

a. Upper panel: Merged images between the phase contrast and the DAPI fluorescent signal of R800-*P_{comX}-rocS* cells in the presence of increasing concentration of ComS inducer (NI=not induced, 0.1, 0.5 and 1 μM). Scale bar, 1 μm. Bottom panel: Cell size parameters are presented as heat maps in which cell width distribution is presented as a function of the cell length of R800-*P_{comX}-rocS* cells. n_T indicates the number of cells analyzed of experiments made in triplicate. **b.** Percentage of anucleate cells for the R800-*P_{comX}-rocS* strains grown in the presence of increasing concentration of ComS. n_T indicates the number of cells analyzed. NI stands for ‘not induced’. Experiments were made in triplicate. Bar chart, with data points overlap, represents the mean ± SEM. Two-tailed P-values derived from a two-population proportion test for the following pairs: ‘WT’ vs ‘NI’ ($P<0.0001$); ‘NI’ vs ‘0.1 μM’ ($P<0.0001$); ‘0.1 μM’ vs ‘0.5 μM’ ($P=3.62 \cdot 10^{-11}$) and ‘0.5 μM’ vs ‘1 μM’ ($P=3.78 \cdot 10^{-1}$). **** $P<0.0001$; ns $P>0.05$. **c.** Western immunoblot of whole-cell lysates from R800-*P_{comX}-rocS* cells, grown to exponential phase in the presence of increasing concentration of ComS inducer (NI=0, 0.1, 0.5 and 1 μM), were probed with anti-RocS antibody. To estimate the relative quantity of proteins in crude extract and to compare the different lanes, we used enolase (Spr1036) as an internal standard. The enolase was detected using specific antibodies (α Enolase) as described in ²⁸ and is presented in the lower part of the figure. Experiments were repeated independently three times with similar results.



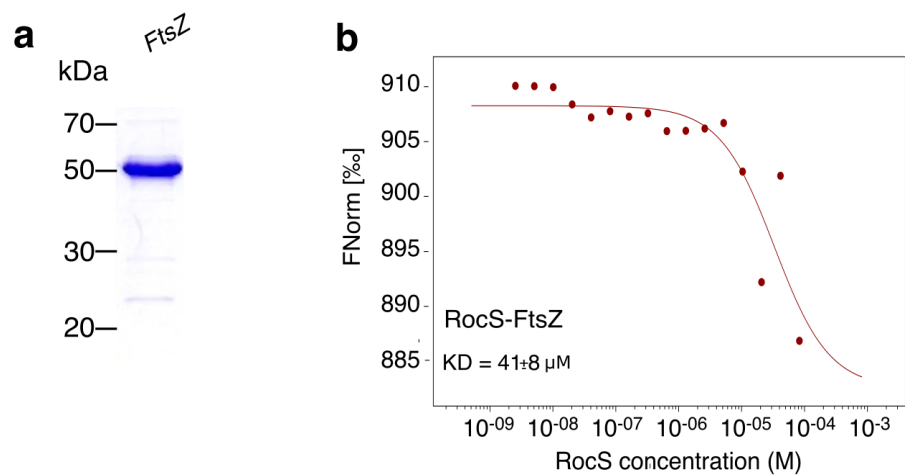
Supplementary Figure 21: Co-localization of CpsD-mKate2 and GFP-RocS in D39 cells

a-b. Heat map representing the longitudinal localization of (a) CpsD-mKate2 or (b) GFP-RocS as a function of the cell length in WT D39 cells expressing both fusions. As already observed in Fig 3a, GFP-RocS first localized at mid-cell and then at the future site of division as the cell elongate, while CpsD-mKate2 localized mostly at mid-cell. The red boxes indicate when both RocS and CpsD co-localize at mid-cell. n indicates the number of cells analyzed. **c.** Representative images of mKate2 and GFP fluorescence signals and phase contrast. The merged image is also shown. Scale bar, 1 μm . Experiments were repeated independently three times with similar results.

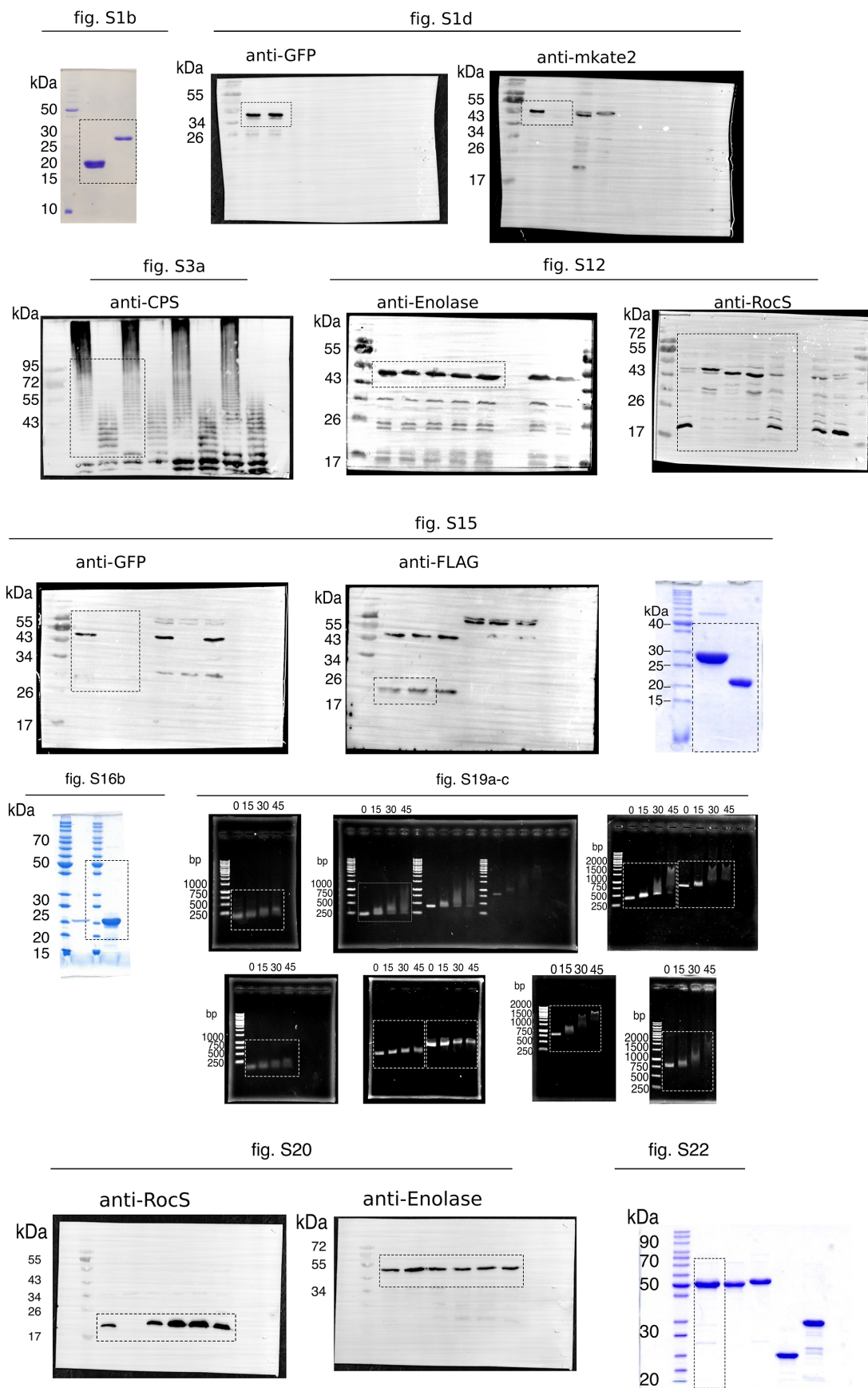


Supplementary Figure 22: Interaction between RocS and FtsZ

a. Purification of FtsZ. After overproduction and purification from *E. coli* cells, FtsZ was analyzed by SDS-PAGE. Experiments were repeated independently three times with a similar purification levels. **b.** Affinity measurements by Microscale Thermophoresis of labeled RocS- Δ AH-6His binding to increasing concentrations of FtsZ. FNorm (normalized fluorescence = fluorescence after thermophoresis / initial fluorescence) is reported on the y-axis and ligand concentrations on the x-axis are plotted in Molar. Measures are represented by blue dots and fitted curves by green lines. Three independent experiments were performed. KD is expressed as the mean \pm SD.



Supplementary Figure 23: Full images of immunoblots and SDS-PAGE used in this study



Supplementary Video 1: Nucleoid segregation in wild-type R800 cells

Time-lapse analysis of HlpA-mKate2 in WT cells. The video shows an overlay of mKate2 (red) and phase-contrast (gray) images. Scale bar: 1 μm . Time interval: 3 min. Experiments were repeated independently three times with similar results.

Supplementary Video 2: Absence of chromosome segregation in $\Delta rocS$ cells

Time-lapse analysis of HlpA-mKate2 in $\Delta rocS$ cells. The video shows an overlay of mKate2 (red) and phase-contrast (gray) images. Scale bar: 1 μm . Time interval: 3 min. Experiments were repeated independently three times with similar results.

Supplementary Video 3: Chromosome pinching in $\Delta rocS$ cells

Time-lapse analysis of HlpA-mKate2 in $\Delta rocS$ cells. The video shows an overlay of mKate2 (red) and phase-contrast (gray) images. Scale bar: 1 μm . Time interval: 3min. Experiments were repeated independently three times with similar results.

Supplementary Video 4: Localization of GFP-RocS

Time-lapse analysis of GFP-RocS in wild-type cells. The video shows an overlay of GFP (green) and phase-contrast (gray) images. White arrowheads highlight bright clusters that remain stationary for at least 3 consecutive frames. Scale bar: 1 μm . Time interval: 100 ms. Experiments were repeated independently three times with similar results.

Table S1 : Strains and plasmids

Strain	Genotype and description	Reference	Primers
<i>S. pneumoniae</i> strains			
R800	R800	35	
$\Delta rocS$	R800 <i>rpsL::rpsL1; ΔrocS</i>	This study	1-3;2-4;5-6
$\Delta HTH\text{-}rocS$	R800 <i>rpsL::rpsL1; rocS::ΔHTH\text{-}rocS</i>	This study	1-3;2-4;15-16
$rocS\text{-}ΔAH$	R800 <i>rpsL::rpsL1; rocS::rocS ΔAH</i>	This study	1-3;2-4;117-18
<i>gfp\text{-}rocS</i>	R800 <i>rpsL::rpsL1; rocS::gfp\text{-}rocS</i>	This study	1-3;2-4;19-20
<i>gfp\text{-}ΔHTH\text{-}rocS</i>	R800 <i>rpsL::rpsL1; rocS::gfp ΔHTH\text{-}rocS</i>	This study	1-3;2-4;21-19
<i>gfp\text{-}rocS\text{-}ΔAH</i>	R800 <i>rpsL::rpsL1; rocS::gfp\text{-}rocS ΔAH</i>	This study	1-3;2-4;19-20
<i>parB\text{-}sgfp\text{-}spc</i>	R800 <i>rpsL::rpsL1; parB::parB\text{-}sgfp\text{-}spc</i>	This study	22-23
<i>hpna\text{-}mKate2</i>	R800 <i>rpsL::rpsL1; hpna::hpna\text{-}mKate2\text{-}cm</i>	16	
<i>hpna\text{-}mKate2\text{-}ΔrocS</i>	R800 <i>rpsL::rpsL1; hpna::hpna\text{-}mKate2\text{-cm}; ΔrocS</i>	This study	1-3;2-4;5-6
<i>flag\text{-}rocS</i>	R800 <i>rpsL::rpsL1; rocS::flag\text{-}rocS</i>	This study	1-3;2-4;5-6;30-31
<i>flag\text{-}rocS\text{-}</i>	R800 <i>rpsL::rpsL1; rocS::flag\text{-}rocS; parB::parB\text{-}sgfp\text{-}spc</i>	This study	22-23
$\Delta rocS\text{-}P_{comX}\text{-}rocS$	R800 <i>rpsL::rpsL1; ΔrocS; ΔIS1167::P1::P_{comR}::comR; cpsN-O::P_{comX}::rocS</i>	This study	7-8;9-10;11-12; 13-14
<i>parS E.f</i>	R800 <i>rpsL::rpsL1; thmA-IS1167::parS E.f</i>	This study	30-31
<i>P_{comX}\text{-}repC\text{-}gfp</i>	R800 <i>rpsL::rpsL1; DIS1167::P1::P_{comR}::comR;</i> <i>cpsN-O::P_{comX}::repC\text{-}gfp</i>	This study	212-14;32-33; 38-39
<i>parS E.f</i>	R800 <i>rpsL::rpsL1; DIS1167::P1::P_{comR}::comR;</i>	This study	9-32;33-
<i>P_{comX}\text{-}repC\text{-}gfp</i>	<i>cpsN-O::P_{comX}::repC\text{-}gfp; thmA-IS1167::parS E.f</i>	This study	14;34-35
$\Delta rocS\text{-}parS E.f$	R800 <i>rpsL::rpsL1; DrocS; DIS1167::P1::P_{comR}::comR;</i>	This study	9-32;23-
<i>P_{comX}\text{-}repC\text{-}gfp</i>	<i>cpsN-O::P_{comX}::repC\text{-}gfp; thmA-IS1167::parS E.f</i>	This study	14-30-31
<i>P_{comX}\text{-}repC\text{-}gfp</i>	R800 <i>rpsL::rpsL1; DrocS; DIS1167::P1::P_{comR}::comR;</i> <i>cpsN-O::P_{comX}::repC\text{-}gfp; thmA-IS1167::parS E.f; rocS::mkate2\text{-}rocS</i>	This study	5-19;20-6
<i>mkate2\text{-}rocS</i>			
R800 <i>dnaA^{ts}</i>	R800 <i>rpsL::rpsL1; dnaA^{ts}</i>	This study	56-57
R800 <i>gfp\text{-}ftsA</i>	R800 <i>ftsA::gfp\text{-}ftsA</i>	This study	58-59;60-61
R800 <i>gfp\text{-}ftsA</i> $\Delta rocS$	R800 <i>gfp\text{-}ftsA, ΔrocS</i>	This study	1-3;2-4;5-6
D39	virulent strain	28	
D39 $\Delta rocS$	D39 <i>rpsL::rpsL1; ΔrocS</i>	This study	1-3;2-4;5-6
D39 $\Delta rocS\text{-}P_{comX}\text{-}rocS$	D39 <i>rpsL::rpsL1; ΔrocS; ΔIS1167::P1::P_{comR}::comR;</i> <i>bbgA::P_{comX}::rocS</i>	This study	11-12-13-14 36-37
D39 $\Delta rocS\text{-}P_{comX}\text{-}rocS$ Δsmc	D39 <i>rpsL::rpsL1; DrocS; DIS1167::P1::P_{comR}::comR;</i> <i>bbgA::P_{comX}::rocS, smc::kan-rpsL</i>	This study	26-27
D39 $\Delta rocS\text{-}P_{comX}\text{-}rocS$ $\Delta parB$	D39 <i>rpsL::rpsL1; DrocS; DIS1167::P1::P_{comR}::comR;</i> <i>bbgA::P_{comX}::rocS, parB::spc</i>	This study	22-23
D39 $\Delta cpsD$	D39 <i>rpsL::rpsL1; ΔcpsD</i>		10
D39 <i>cpsD\text{-}3YF</i>	D39 <i>rpsL::rpsL1; cpsD::cpsD\text{-}3YF</i>		10
D39 <i>cpsD\text{-}3YF\text{-}ΔrocS</i>	D39 <i>rpsL::rpsL1; cpsD::cpsD\text{-}3YF; ΔrocS</i>	This study	1-3;2-4;5-6
D39 <i>cpsD\text{-}3YF\text{-}ΔparB</i>	D39 <i>rpsL::rpsL1; cpsD::cpsD\text{-}3YF; parB::spc</i>	This study	22-23
D39 <i>cpsD\text{-}3YE</i>	D39 <i>rpsL::rpsL1; cpsD::cpsD\text{-}3YE</i>		10
D39 <i>cpsD\text{-}3YE\text{-}ΔrocS</i>	D39 <i>rpsL::rpsL1; cpsD::cpsD\text{-}3YE; ΔrocS</i>	This study	1-3;2-4;5-6
D39 <i>cpsD\text{-}mkate2</i>	D39 <i>rpsL::rpsL1; cpsD::cpsD\text{-}mkate2</i>		10
D39 <i>cpsD\text{-}mkate2</i> $\Delta gfp\text{-}rocS$	D39 <i>rpsL::rpsL1; cpsD::cpsD\text{-}mkate2; rocS::gfp\text{-}rocS</i>	This study	1-3;2-4;19-20
D39 Δcps	D39 Δcps		29
D39 $\Delta cps\text{:rpsL1}$	D39 $\Delta cps, rpsL::rpsL1$	This study	28-29
D39 $\Delta cps\text{:rpsL1}$ $\Delta rocS$	D39 $\Delta cps, rpsL::rpsL1, ΔrocS$	This study	1-3;2-4;5-6
<i>E. coli</i> strains			
XL1-Blue	<i>supE44 hsdR17 recA1 endA1 gyrA46 thi relA1 lac⁻</i>	30	
	<i>F'[proAB⁺ lac]^q lacZ ΔM15 Tn10 (Tc^R)</i>		
BL21 (DE3)	<i>F- ompT gal dcm lon hsdS_B (r_B-m_α-)</i>	31	
	<i>λ (DE3 [lacI lacUV5-T7 gene lind sam7 nin5])</i>		
Plasmids			
pT7.7	pT7.7 derivative, encoding a His-tag for C-terminal fusions	34	
pT7.7 <i>parB</i>	pT7.7 derivative, encoding <i>par</i> , from Met1 to Lys252	10	
pT7.7 <i>rocS\text{-}ΔAH</i>	pT7.7 derivative, encoding <i>rocS</i> , from Met1 to Gln150	This study	65-66
pT7.7 <i>rocS\text{-}G15P</i>	pT7.7 derivative, encoding <i>rocS</i> , from Met1 to Gln150 with one mutation Gly15 to Pro	This study	62-66
pT7.7 <i>ftsZ</i>	pT7.7 derivative, encoding <i>ftsZ</i> , from Met1 to Arg442	This study	63-64
pQE30	pQE30 derivative, encoding a <i>his-tag</i> for N-terminal fusion	Qiagen	
pQE30 <i>cpsC/D TIGR4</i>	pQE30 derivative, encoding <i>CpsD</i> , from Met1 to Lys227, fused to the C-terminal part of <i>CpsC</i> , from Leu200 to Lys230 pGBDU derivative, encoding binding domain of <i>gal4</i> for N-terminal fusions, <i>ura3</i>	10	
pGBDU-C1		37	
pGBDU-C1- <i>cpsD</i>	pGBDU derivative, encoding <i>cpsD</i> , from Met1 to Lys226	10	
pGBDU-C1- <i>cpsC</i>	pGBDU derivative, encoding <i>cpsC</i> , from Met1 to Lys230	10	
pGAD-C1	pGAD derivative, encoding activation domain of <i>gal4</i> for N-terminal fusion, <i>leu2</i>	10	
pGAD-C1- <i>cpsD</i>	pGAD derivative, encoding <i>cpsD</i> , from Met1 to Lys226	10	
pGAD-C1- <i>cpsC</i>	pGAD derivative, encoding <i>cpsC</i> , from Met1 to Lys230	10	

Table S2 : List of Primers

Forward and reverse primers are represented by plus (+) or minus (-), respectively

Number	Name	séquence 5'-3'
1	Upstream of <i>rocS</i> (+)	GCTGCTATGAGTGGCGATTGGC
2	Downstream of <i>rocS</i> (-)	CTACTTCCTGCTCTAACAACTCCCTAG
3	Upstream of <i>rocS</i> / Janus (-)	CATTATCCATAAAAATCAAACGGAATATCCTCTGAAACGTTTCTAGC
4	Janus / Downstream of <i>rocS</i> (+)	GGAAAGGGGCCAGGTCTTCAGGAGCTTTAGGTTAAATGC
5	Δ <i>rocS</i> (+)	TCAAGGAGCTGTTAGGTAAATGC
6	Δ <i>rocS</i> (-)	GCATTTAACCTAACAGCTCTGAAATATCCTCTGAAACGTTTCTAGC
7	SG258	CATCGAACCTATACTCTTTAG
8	SG261	ATAACAAATCCAGTAGCTTTGG
9	<i>treR-up</i>	ATGAAGAACATAACAAATTAAAGCAAATCC
10	<i>amf-up</i>	GCCITGTTTCAAGGGTACCAAT
11	<i>cpsN / rocS</i> (+)	ATTTATTTTATTGAGGTTCAATGAGTATTGAATGACC
12	<i>cpsN</i> O (-)	TTTCAATATGTAACTCTCCCAT
13	<i>rocS</i> / <i>P_comX</i> (-)	ATGGGAAGAGTTACATATTAGAAATTATCCTCCAAATAACGAGCAA
14	<i>P_comX.ther</i> (+)	TGAACCTCCAATAAAATATAAT
15	Δ <i>N ter-rocS</i> (+)	GTTTCAGAGGATTTATGAGTATTGAAATTACCAAGAGACAGATAAAAAT
16	Δ <i>N ter-rocS</i> (-)	AATACTTAAATATCTCTGAAACGTTTGTACCTAG
17	<i>rocS</i> Δ <i>Cter</i> (+)	GCAAAAGAAGAAGTCCAATCCACTTAATCAAGGAGCTTTAGGTTAAATG
18	<i>rocS</i> Δ <i>Cter</i> (-)	AGTGATTGGACTTCTCTTTTC
19	<i>gfp-rocS</i> (-)	CTTCACCTTGAAGAACATAATATCCTCTGAAACGTTTTC
20	<i>gfp-rocS</i> (+)	CTCGAGGGATCCGAATGAGTATTGAAATGACC
21	<i>gfp- N ter-rocS</i> (+)	CTCGAGGGATCCGAATGAGTATTGAAATGACC
22	Upstream of <i>parB</i> (+)	CTGACACTTCTCTGATATTGC
23	Downstream of <i>parB</i> (-)	GGGATATTTAACACGGCATTAGG
24	Upstream of <i>hlpA</i> (+)	CGAAGTTAGCTCAAGAAG
25	Downstream of <i>hlpA</i> (-)	CAGTTGATTTATGAG
26	<i>smc</i> (+)	TTATGCCATGAGCACGCCCTTAAAGATTC
27	<i>smc</i> (-)	CTAATTCACAAATAGCTACACCTTATCGACAT
28	<i>rpsL</i> (+)	CTATATCAGTATAGCATGTAG
29	<i>rpsL</i> (-)	CTTCAGCCATACGGTAGATTC
30	<i>flag rocS</i> (+)	GACTACAAAGACCATGACGGTGAATTAAAGATCATGATATCGACTACAAAGATGACGACGATAACTGAGGGATCCGAATGAGTATTGAATGACC
31	<i>flag rocS</i> (-)	TCGGGATCCCTGAGTTATCGTCATCTTGTAGTCGATATCATGATCTTATAACCGCTATGGTCTTGTAGTCATAATCCTCTGAAACGTTTTC
32	<i>cpsN</i> / <i>repC</i> (+)	ATTTTATTTATTGAGGTTCAATGAGTAAGTATACTTC
33	<i>repC</i> / <i>P_comX</i> (-)	ATTGGGAAGAGTACATATTAGAAATTATTTATAACATTAC
34	<i>parS E.f</i> (+)	GTTATTGAAATACGGTTAC
35	<i>parS E.f</i> (-)	CTTCCCACGCCCTTTG
36	<i>bgaA</i> (+)	GGTTTTGACTCTATCTCGCTTATTTAATTG
37	<i>bgaA</i> (-)	GCCGGCTGTATCTAGGATAC
38	<i>repC E.f</i> (+)	CCATTATTTAACACAGGGTCTACCATGAGTAAGTTACATTCA
39	<i>repC E.f</i> (-)	CTGAGGAACCTGGATGTCAGTTTTTTGTTCTTTGTCG
40	DNA 50 pb (+)	TGTTGCCATTGCTACAG
41	DNA 50 pb (-)	GCCATACAAACGACG
42	DNA 100 pb (+)	CGCCAGTTATAGTTGCG
43	DNA 100 pb (-)	TCGTTGGAAACCG
44	DNA 200 pb (+)	CGCCCTCATCCAGTCTATTAAATTG
45	DNA 200 pb (-)	GAGCTAACCGCTTTTGAC
46	DNA 400 pb (+)	CAATGATACCGGGAGACCCAG
47	DNA 400 pb (-)	TACGGGATGGCATGACAGTAAG
48	DNA 800 pb (+)	CTAGATCTTTAAATTTAAATG
49	DNA 800 pb (-)	TCGAACCTGGATCTAACAG
50	DNA <i>P.aeruginosa</i> (+)	GCTGCCAGCCGCCGAGC
51	DNA <i>P.aeruginosa</i> (-)	GAACGGCTGCAGGTAGCTAG
52	<i>qPCR_parB</i> (+)	ACGGTCTATCCAGCTGTTG
53	<i>qPCR_parB</i> (-)	ATAGGGCGGTCTCTCTA
54	<i>qPCR_ter</i> (+)	AAAAAGTACCATCCCCAGCA
55	<i>qPCR_ter</i> (-)	AGCCTTGGCTCATCATTG
56	<i>dnaA_T1193C</i> (+)	TCAAGTAGCCAGCTTTATCTAGAG
57	<i>dnaA_T1193C</i> (-)	CTAGATAAAATACGTGGCTACTTGAC
58	<i>ftsA-kan-rpsL</i> (+)	CATTATCCATAAAAATCAAACGGTACATCGCTCTCTATCTTCC
59	<i>ftsA-kan-rpsL</i> (-)	GGAAAGGGGCCAGGTCTAGAGGAAAATAATTGACATTTCATTG
60	<i>gfp-ftsA</i> (+)	GTATAAAACTCGAGGGATCCGAATGCTAGAGAAGGTTTTCAAG
61	<i>gfp-ftsA</i> (-)	CAATTCTCACCTTAGAAATCATTACATCGCTCTCTATCTTCCAG
62	<i>pT7.7 rocs-G15P</i>	TATCATATGAGTATTGAAATGACCGTCAGTGAAGATTGAGGGTACCGTACCTTACCGTACATCAAAACCGT
63	<i>pT7.7 ftsZ</i> (+)	ACATTTTCATTTGATACAG
64	<i>pT7.7 ftsZ</i> (-)	AACGATTTTGAAGGAAATGG
65	<i>pT7.7 rocs</i> Δ <i>Cter</i> (+)	TATCATATGAAAGACAGATAAAATGACAAGAGG
66	<i>pT7.7 rocs</i> Δ <i>Cter</i> (-)	TATCTGCAGTTAAGTGGACTTCTCT